JOURNAL OF MATERIALS SCIENCE 25 (1990) 1856–1862

A study on age hardening in cast Fe–Mn–Al–Si–C alloys

A. PRODHAN, A. K. CHAKRABARTI
Department of Metallurgical Engineering, Indian Institute of Technology, Kharagpur-721302, India

Phase transformations in a group of cast and solution treated (at 1100° C) Fe–Mn–Al–Si–C alloys during isothermal ageing have been investigated as a function of (a) ageing temperature (500 to 800° C), (b) aluminium (5 to 10%) and carbon (0.27 to 0.9%) contents for fixed manganese (~30%) and silicon (~1.5%) levels. Irrespective of the ageing temperature and carbon content, 5% Al alloys do not undergo appreciable ageing. Ageing tendency increases with increase in aluminium and carbon contents. Hardening is caused by the precipitation of Al(Fe, Mn)C_x phase inside the austenite grain and $Mn_{12}Si_7Al_5$ phase at the grain boundaries. The sequence of precipitation of the phases depends on the ageing temperature and composition. Cold working by rolling, after homogenization at 1100° C, accelerates ageing.

1. Introduction

Phase transformation in Fe–Mn–Al alloys during isothermal and isochronal ageing have been studied by several investigators [1–13] in the past. Such investigations have been conducted mainly on homogenized and wrought materials. Hardly any study was made on cast alloys. Moreover, different groups had worked on alloys of widely varying compositions which in most cases did not include silicon. Although there is a general agreement on the ageing behaviour of Fe–Mn–Al alloys, it is obvious from a scrutiny of the literature that no definite trend regarding the effect of composition on the relative ageing response of Fe–Mn–Al alloys has emerged from the past investigations. The present investigation was aimed at studying the phase transformation in a group of cast alloys during isothermal ageing as a function of (a) transformation temperature, (b) aluminium (5 to 10%) and (c) carbon (0.27 to 0.9%) contents for fixed manganese (~30%) and silicon (~1.5%) levels. Silicon is known to improve oxidation and corrosion resistance and mechanical properties of Fe–Mn–Al alloys. Silicon also improves castability of alloy steels. Hence the cast alloy compositions investigated included silicon. The basic characteristic of transformations in Fe–Mn–Al–Si–C alloys is highlighted in the present paper.

2. Experimental procedure

The alloys for the present series of investigations were prepared in an air induction furnace (1.5 kg capacity) under CaO–CaF_2 flux cover. For all the melts, the charge consisted of mild steel scrap, low and high carbon ferromanganese, ferrosilicon and aluminium. The compositions of the alloys are given in Table I. The cast samples (10 mm × 10 mm × 150 mm) were homogenized at 1100° C for one hour. The samples were cooled by forced air draft after homogenization. The ageing tendencies of cast, homogenized and forced air draft quenched samples Fe–Mn–Al alloys were investigated. Approximately 10 mm × 10 mm × 4 mm samples were aged at temperatures of 500° C, 600° C and 800° C for periods ranging from 10 to 10 000 min. Samples of alloys 1A, 1C, 2A, 2C, 3A and 3C were also cold rolled and aged at 600° C. The progress of the ageing reaction was followed by hardness measurements. Precipitates formed at different stages of ageing were identified by X-ray diffraction (XRD) using Cu-K_α (λ = 0.154 nm) radiation. Morphology of the precipitates in the overaged samples was also investigated by scanning electron microscopy (SEM) and optical microscope.

3. Results

In as-homogenized condition the matrices in all the samples were free from any precipitate. In the 5% Al alloys, the matrix was almost fully austenitic. In the higher aluminium alloys, duplex austenite–ferrite matrix formed. The proportion of austenite and ferrite in each case depended upon the actual composition [14]. Representative microstructures of homogenized samples are shown in Fig. 1.

TABLE I Chemical composition of alloys

Alloy code	% Mn	% Al	% Si	% C	% Fe
1A	30	5.5	1.7	0.27	
1B	32	5.2	1.7	0.55	
1C	31.2	5.4	1.67	0.92	
2A	29.34	8.0	1.65	0.27	
2B	31.5	7.8	1.55	0.57	Balance
2C	32.1	7.4	1.58	0.89	
3A	30.25	9.5	1.5	0.29	
3B	30.5	9.7	1.5	0.6	
3C	30.5	9.8	1.47	0.91	

0022–2461/90 $03.00 + .12

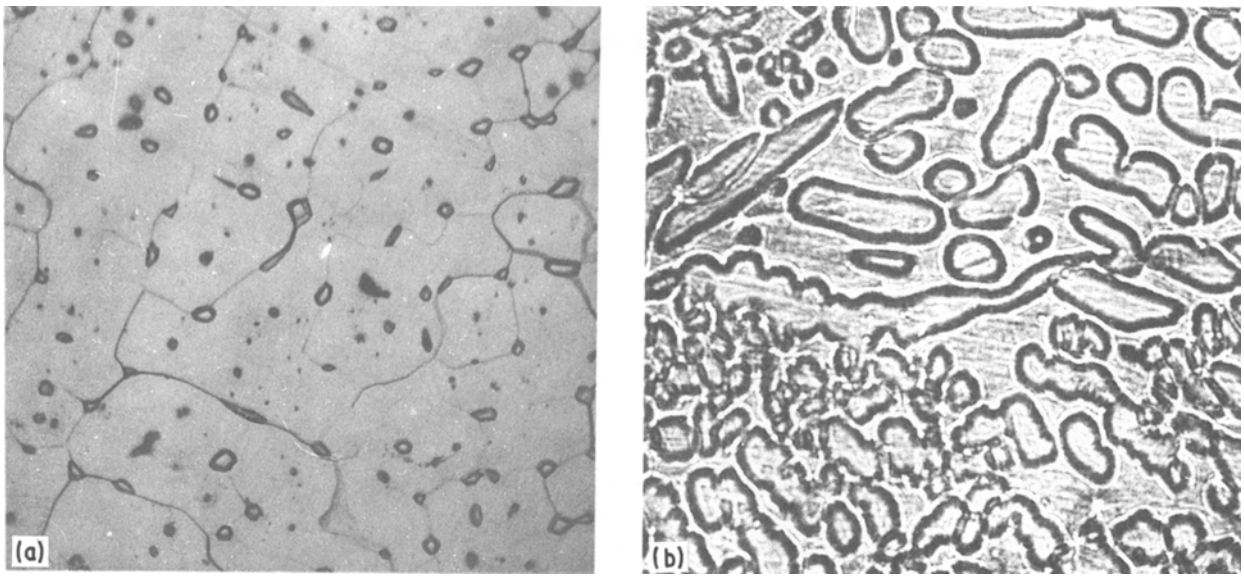

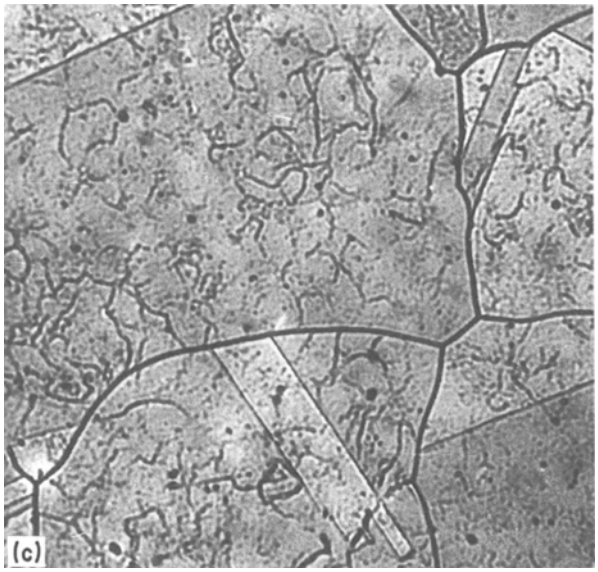

Figure 1 Microstructures of homogenized (at 1100° C) samples of (a) alloy 1A (5Al, 0.3 C); (b) alloy 3A (10 Al, 0.3 C); (c) alloy 3C (10 Al, 0.9 C). Magnification 200 ×.

The effect of phase transformation during isothermal ageing can be appreciated most conventionally from the hardness against ageing time plots. The isothermal ageing curves for different alloys are given in Figs 2 to 4. Depending on aluminium and carbon contents, the alloys responded to ageing treatment to a varying degree. From the ageing curves, the following trends could be noted:

1. The alloys containing 5% Al responded only mildly to ageing treatment (Fig. 2).

2. The alloys with 7.5% Al and 10% Al responded appreciably to ageing treatment. The extent of hardening increased with increase in carbon content from 0.3% to 0.9%. But the extent of hardening was conspicuously lower in alloys with 0.6% C (Alloys 2B and 3B). Most of the ageing curves show multiple peaks (Fig. 3 and 4).

3. Prior deformation of homogenized samples by cold rolling accelerated ageing (Figs 2 to 4).

4. The variation of hardness was maximum in the ageing temperature range 500° to 600° C. At 800° C the extent of ageing was not appreciable in most of the alloys.

Profuse precipitation of carbide and intermetallic phases occurred on ageing particularly in the temperature range 500° C to 600° C. The phases identified by XRD are given in Table II. The data suggest the existence of two major types of precipitate phases – $[Al(Fe, Mn)_3C_x]$ and $[Mn_{12}Si_7Al_5]$. Metallographic examination of alloy 3C aged at 800° C showed precipitation mainly along austenite grain boundaries (Fig. 5a). At lower ageing temperatures, precipitation had occurred both at the austenite grain boundaries as well as inside the austenite grains (Figs 5b and 5c). SEM examination of aged samples further revealed that the carbide precipitate particles were mainly rod like, but in some of the samples the rod like precipitates had undergone partial spheroidization (Fig. 6).

4. Discussion

The study has confirmed the general scheme of phase transformations in Fe–Mn–Al alloys suggested by

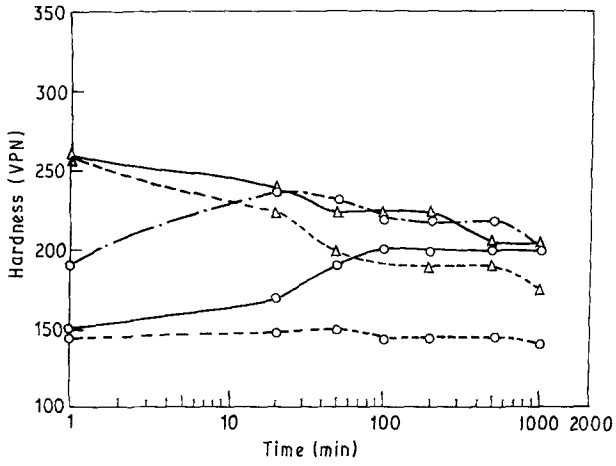

Figure 2 Ageing response of alloys with 5% Al (alloy 1A, 0.3% C, alloy 1B, 0.6% C; alloy 1C, 0.9% C) at 600° C. ○ Solution treated and aged; △ Solution treated, rolled (30% deformed) and aged — — 0.3% C; - - - 0.6% C; —— 0.9% C.

earlier workers [1–13]. However, in addition to confirming earlier results the present study has thrown new light on the following aspects of ageing behaviour of Fe–30Mn–(5–10)Al–(0.3 to 0.9)C–1.5Si alloys:

1. Effect of compositional variables on response to ageing treatment at various temperatures.

2. Morphology and distribution of precipitates and sequence of precipitation. The results are discussed in details in the following sections.

4.1. Ageing response of the alloys

At 800° C appreciable ageing tendency was observed only in alloy 3C. From phase analysis (Table II) and metallography (Fig. 5) it is clear that the hardening was caused by precipitation of $Mn_{12}Si_7Al_5$ phase mainly at the grain boundary regions. The volume fraction of $Mn_{12}Si_7Al_5$ phase was not appreciable in the other alloys aged at 800° C. This explains their comparative lack of response to ageing.

At 600° C, hardness increase on ageing of alloys 2A, 2B, 2C, 3A and 3C was appreciable. The ageing curves for alloys 2A and 2C (Fig. 3b) show two peaks whereas alloys 3A and 3C show only one peak (Fig. 4b). On the basis of phase analysis data reported in Table II, initial hardening of alloys with 7.5% Al (2A and 2C) may be attributed to the precipitation of a carbide phase. The drop in hardness in the ageing curve after the first peak was presumably caused by coarsening of the carbide precipitates. However, onset of $Mn_{12}Si_7Al_5$ precipitates again caused hardening. In the as-rolled samples, initial hardness was higher. The dislocations presumably provided ample sites for precipitation of carbide. Although dislocations are likely to be annihilated during ageing at 600° C, it is possible that the fine dispersion of carbide precipitate throughout the matrix contributed to additional hardening. The effect of prior deformation on ageing was even more conspicuous in alloy 2A. Under normal homogenized condition, the ageing response in the alloy was mild. However, when the same alloy was aged after cold rolling, a strong ageing peak was observed. In alloys 3A and 3C precipitation of carbide and $Mn_{12}Si_7Al_5$ phases occurred almost simultaneously. The enhanced response to ageing with increase in aluminium content is quite conspicuous. Since the precipitation of the two phases occurred almost simultaneously, only one peak appeared. Extent of precipitation in alloy 1A was practically nil. The precipitation was small in alloys 2B and 3B. Hence these alloys responded only mildly to ageing. The 500° C ageing curves of both 7.5% and 10% Al series of alloys show multiple hardening peaks on ageing (Figs 3c and 4c). A combined examination of the ageing curves and the phase analysis data (Table II)

TABLE II XRD analysis of different phases on ageing

Temperature °C	Alloy code	Time of exposure (min)	Phases identified with relative intensity
800° C	1C	50	γ(s)
		200	γ(s)
	2C	20	γ(s)
		200	γ(s)
	3C	50	γ(s), α(s)
		200	γ(s), $Mn_{12}Si_7Al_5$(s)
600° C	1A	1000	γ(s), α(w), Al(Fe, Mn)$_3C_x$(w)
	1B	100	γ(s), Al(Fe, Mn)$_3C_x$(w)
		1000	γ(s), α(w), Al(Fe, Mn)$_3C_x$(m)
	1C	1000	γ(s), Al(Fe, Mn)$_3C_x$(s)
	2A	20	γ(s), α(s), Al(Fe, Mn)$_3C_x$(w)
		1000	γ(s), α(s), Al(Fe, Mn)$_3C_x$(s), $Mn_{12}Si_7Al_5$(s)
	2B	2000	γ(s), α(m), Al(Fe, Mn)$_3C_x$(s), $Mn_{12}Si_7Al_5$(m)
	2C	100	γ(s), α(w), Al(Fe, Mn)$_3C_x$(w)
		1000	γ(s), Al(Fe, Mn)$_3C_x$(s), $Mn_{12}Si_7Al_5$(m)
	3A	100	γ(s), α(s), Al(Fe, Mn)$_3C_x$(w), $Mn_{12}Si_7Al_5$(w)
		1000	γ(s), α(s), Al(Fe, Mn)$_3C_x$(s), $Mn_{12}Si_7Al_5$(s)
	3B	50	γ(s), α(s), Al(Fe, Mn)$_3C_x$(w)
		2000	γ(s), α(m), Al(Fe, Mn)$_3C_x$(m), $Mn_{12}Si_7Al_5$(w)
	3C	100	γ(s), α(s), Al(Fe, Mn)$_3C_x$(w), $Mn_{12}Si_7Al_5$(w)
		1000	γ(s), α(m), Al(Fe, Mn)$_3C_x$(s), $Mn_{12}Si_7Al_5$(s)
500° C	2A	200	γ(s), α(s), Fe_3Al(s)
		1000	γ(a), α(s), Fe_3Al(s), Al(Fe, Mn)$_3C_x$(m)
		10000	γ(s), α(s), Fe_3Al(s), Al(Fe, Mn)$_3C_x$(m), $Mn_{12}Si_7Al_5$(m)
	2B	200	γ(s), α(w), Al(Fe, Mn)$_3C_x$(w), $Mn_{12}Si_7Al_5$(w)
		1000	γ(s), α(s), Fe_3Al(s), Al(Fe, Mn)$_3C_x$(m)
		10000	γ(s), α(s), Fe_3Al(w), Al(Fe, Mn)$_3C_x$(m), $Mn_{12}Si_7Al_5$(m)
	2C	5000	γ(s), α(s), Fe_3Al(m), α(m), Al(Fe, Mn)$_3C_x$(m), $Mn_{12}Si_7Al_5$(w)
	3A	200	γ(s), α(s), Fe_3Al(s)
		5000	γ(s), α(s), Fe_3Al(s), Al(Fe, Mn)$_3C_x$(m), $Mn_{12}Si_7Al_5$(m)
	3B	200	γ(s), α(s), Fe_3Al(s)
		10000	γ(s), Fe_3Al(s), α(s), Al(Fe, Mn)$_3C_x$(m), $Mn_{12}Si_7Al_5$(m)

s = strong, m = medium, w = weak

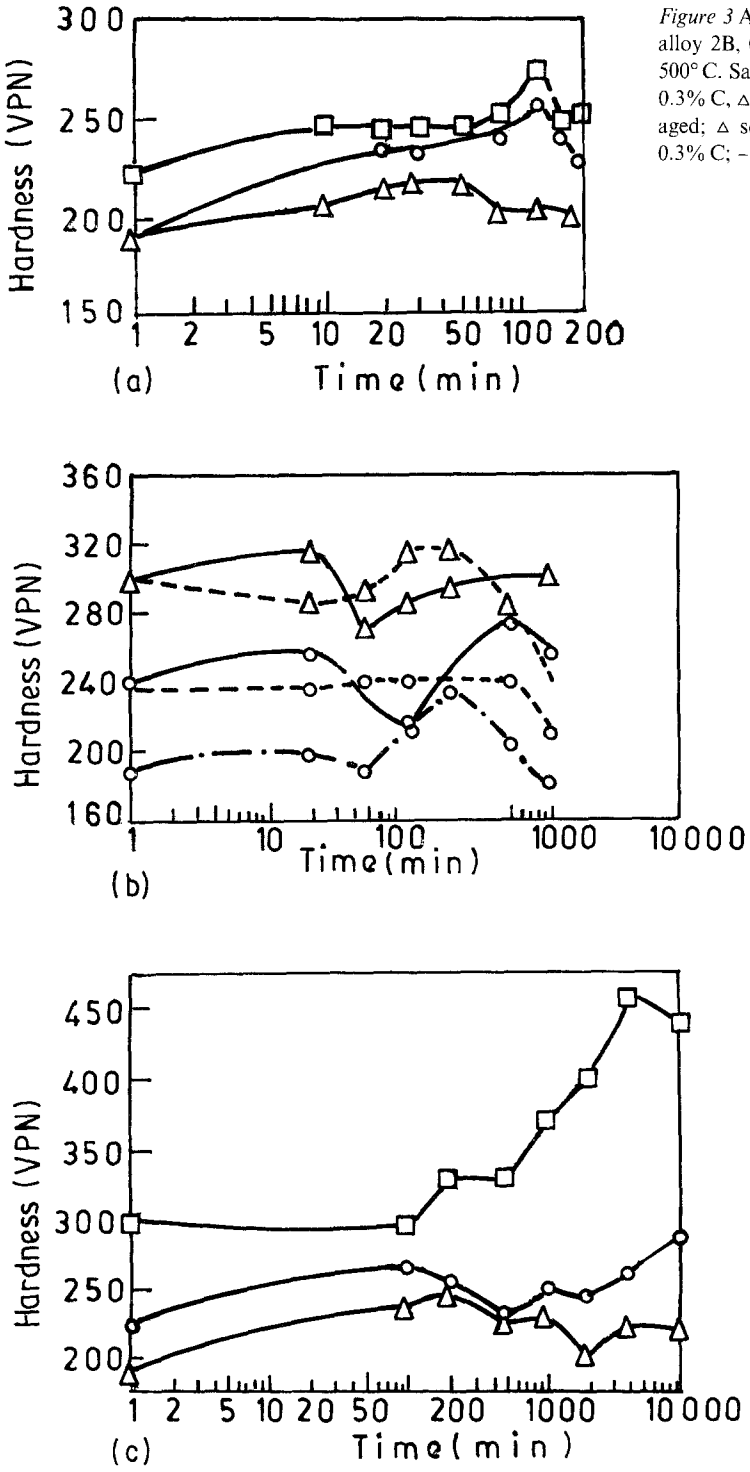

Figure 3 Ageing response of alloys with 7.5% Al (alloy 2A, 0.3% C; alloy 2B, 0.6% C; alloy 2C, 0.9% C) at (a) 800° C; (b) 600° C; (c) 500° C. Samples in (a) and (c) in solution treated condition with ○ 0.3% C, △ 0.6% C, □ 0.9% C. Samples in (b) ○ solution treated and aged; △ solution treated, rolled (30% deformed) and aged. — — 0.3% C; - - - 0.6% C; —— 0.9% C.

suggests that the transformations likely to be responsible for the hardening peaks were as follows:

Stage I : Ordering reaction leading to the formation of Fe_3Al superlattice.
Stage II : Precipitation of complex carbides.
Stage III: Coarsening of carbide precipitates and precipitation of $Mn_{12}Si_7Al_5$ phase.

In most pf the alloys however stages II and III overlapped due to simultaneous precipitation of carbide and $Mn_{12}Si_7Al_5$ phase. In alloy 2C, the volume fraction of precipitate was large and as a result ageing curves rose sharply. It would be interesting to note that alloys 3B (10 Al, 0.6 C) and 2B (7.5 Al, 0.6 C) responded only mildly to ageing treatment even at 500° C.

4.2. Morphology and distribution

Microstructural examination of samples indicated that the $Mn_{12}Si_7Al_5$ phase precipitated at the austenite boundaries (Fig. 5). The carbide precipitates on the other hand formed within the austenite grains in alloys 2A, 2C, 3A and 3C. In alloy 3B appreciable carbide precipitation did not occur within the austenite phase. However, precipitation of some phase within the ferrite grains and $Mn_{12}Si_7Al_5$ phase at ferrite/austenite boundary was observed (Table II). Contrary to earlier reports [8] grain boundary precipitation of carbides was not observed in any of the alloys. The morphology of the carbide precipitates in overaged samples varied from rod like to spheroidized depending upon the extent of coarsening. Carbide precipitates were coarsest and precipitate denisty was maximum in alloy 3C (10

Al, 0.9 C) aged at 500° C (Fig. 6c). The microstructure of the rolled and aged samples of alloy 2A was full of intersecting slip lines on which carbide precipitation had occurred. The intersecting slip lines are generated by slipping on more than one set of planes (Fig. 5c). The microstructure of the cold worked samples resemble the work hardened samples of Hadfield Manganese Steel [15]. The effect of cold working on the mode of precipitation and precipitate morphology can be appreciated from the SEM photographs of alloy 3A given in Figs 6a and b, and the optical micrograph of alloy 3A given in Fig. 5b. For example, in solution treated condition rod like precipitates in alloy 3A were oriented from the grain boundaries into grain bodies (Fig. 6a). At places partial spheroidization of the rod like precipitates had also occurred. In the cold worked sample of the same alloy and under identical conditions of ageing, precipitation had occurred in a more dispersed form throughout the matrix. Most of the precipitate particles were spheroidized. The optical micrograph of the cold worked and aged sample of alloy 3A (Fig. 5b) clearly reveals a cellular pattern of precipitation which occurred probably because of precipitation on subgrain boundaries.

Increase in aluminium thus affects the work hardening mechanism which in turn influences precipitation kinetics and precipitate morphology. Twin formation in Fe–8.25 Al–29.95 Mn–0.85 C alloy under fatigue stress was reported earlier [16]. The phenomenon was attributed to low stacking fault energy [15]. In the present series of alloys the twinning tendency is restricted to 5% Al alloys only. Aluminium has much higher stacking fault energy (200 ergs cm^{-2}) than austenitic stainless steels (13 ergs cm^{-2}) [17]. On increasing the aluminium content to 7.5%, stacking fault energy is increased and the predominant deformation mode changes to slipping. Dislocation cells are probably formed through interaction. The slip lines and cells act as favoured sites for carbide precipitation during ageing. Consequently, ageing process is enchanced.

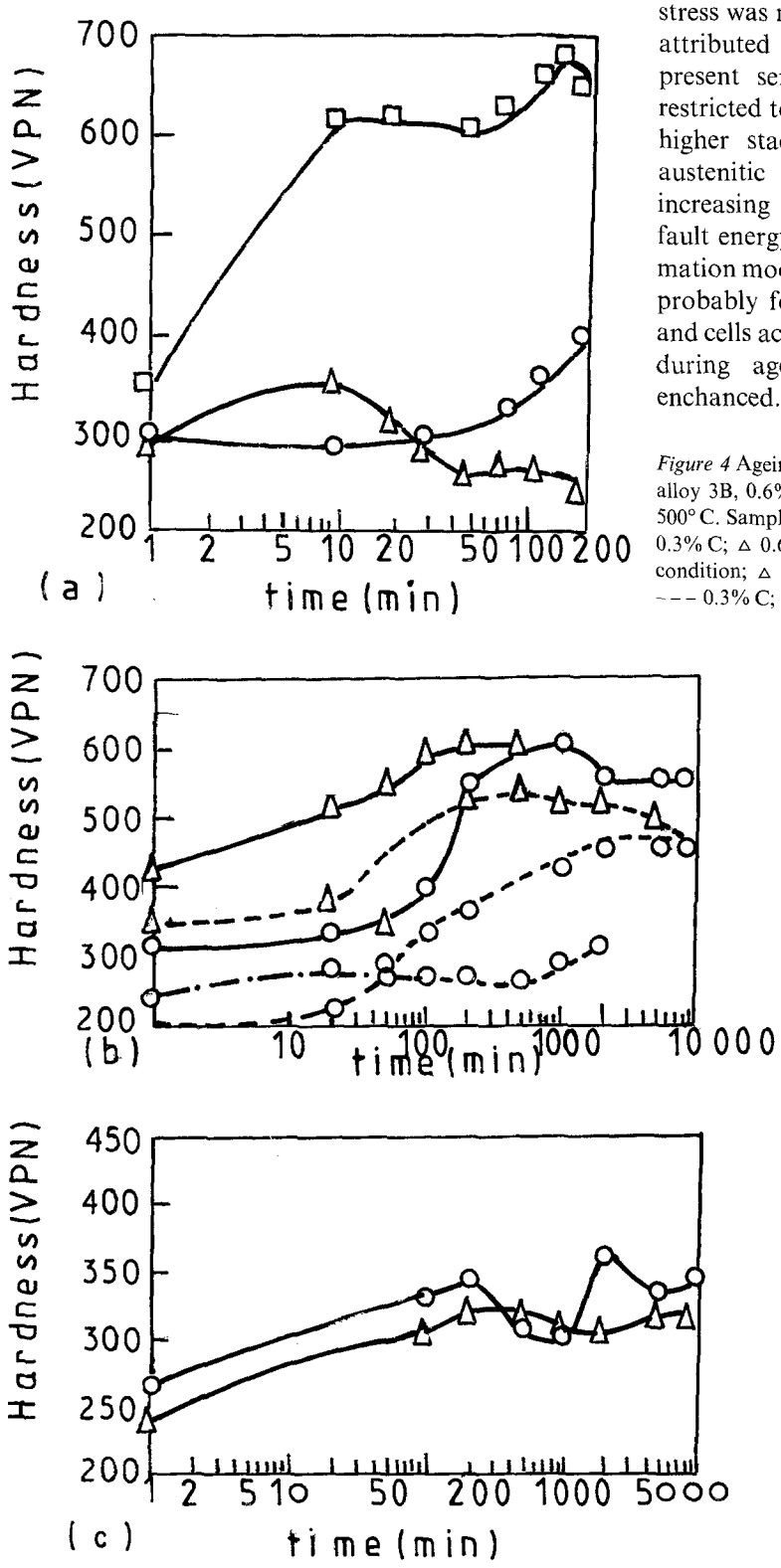

Figure 4 Ageing response of alloys with 10% Al (alloy 3A, 0.3% C; alloy 3B, 0.6% C; alloy 3C, 0.4% C) at (a) 800° C; (b) 600° C; (c) 500° C. Samples in (a) and (c) in solution treated condition with ○ 0.3% C; △ 0.6% C; □ 0.9% C. Samples in (b) ○ solution treated condition; △ solution treated, rolled (30% deformed) and aged. – – – 0.3% C; – – – 0.6% C; —— 0.9% C.

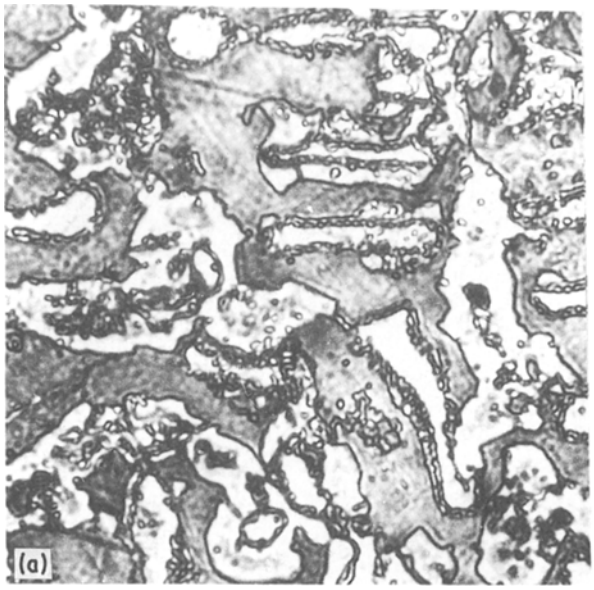

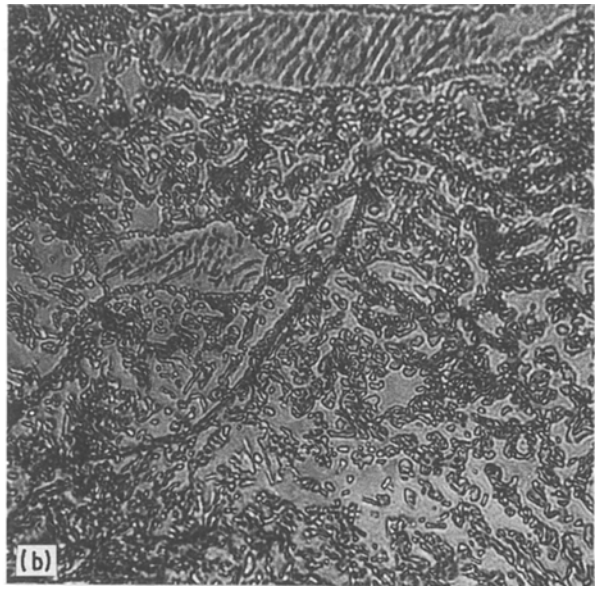

Figure 5 Microstructures of homogenized (at 1100° C) and aged samples of (a) alloy 3C (10% Al, 0.9% C) at 800° C for 200 min and with 30% deformation; (b) alloy 3A (10% Al, 0.3% C); (c) alloy 2A (7.5% Al, 0.3% C) at 600° C for 1000 min. Magnification 500 ×.

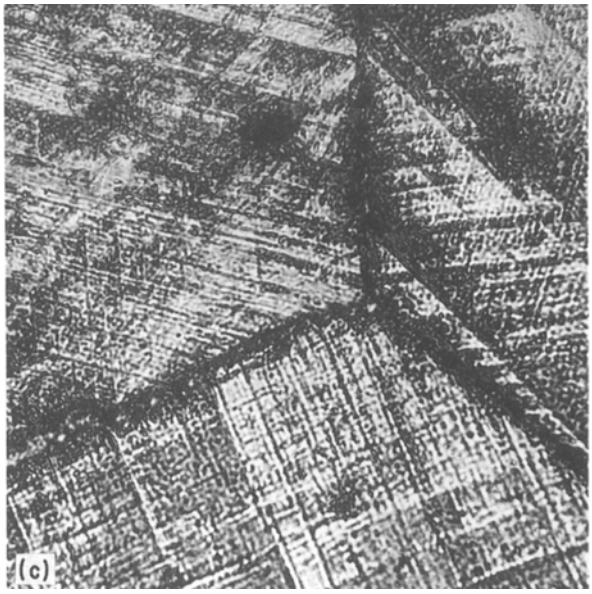

Figure 6 SEM photographs of homogenized (at 1100° C) and aged samples of (a) alloy 3A (10% Al, 0.3% C) at 600° C for 1000 min; (b) alloy 3A cold worked (30% deformation) at 600° C for 1000 min; (c) alloy 3C (10% Al, 0.9% C) at 500° C for 5000 min.

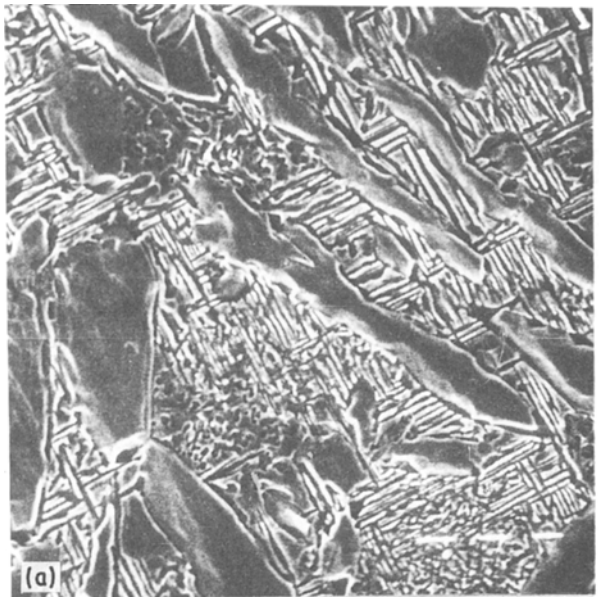

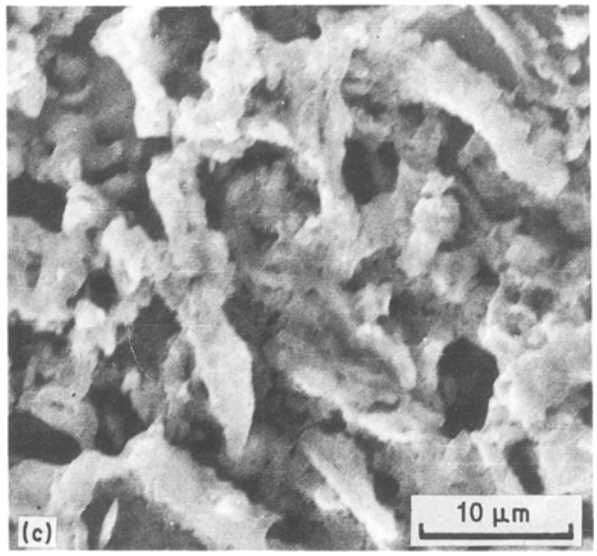

5. Conclusions

1. An Fe–30Mn–5Al–1.5Si–0.3C alloy undergoes only mild ageing at 600° C. The ageing response increases to a little extent when the carbon content is increased from 0.3 to 0.9% keeping the concentration of other alloying elements approximately constant.

2. Fe–30Mn–(7.5–10)Al–1.5Si–C alloys with 0.3% C and 0.9% C are most susceptible to age hardening in the temperature range 500 to 800° C. The same group of alloys with 0.6% C however undergo relatively lower degree of age hardening.

3. The sequence of precipitation of Al(Fe, Mn)C_x and $Mn_{12}Si_7Al_5$ phases depends on the ageing temperature and composition. At 800° C only $Mn_{12}Si_7Al_5$ phase precipitated at grain boundaries in alloy 3C (10Al, 0.9C): carbide precipitation did not occur at 800° C. At lower temperatures e.g. 500° C and 600° C precipitation of the carbide phase preceded the formation of the $Mn_{12}Si_7Al_5$ phase in alloys 2A (7.5Al, 0.3C) and 2C (7.5Al, 0.9C). In the alloys with 10% Al (3A and 3C), precipitation of both the phases occurred almost simultaneously.

4. Cold working by rolling accelerates ageing.

5. Carbide precipitation occurs throughout the austenite matrix. Carbide morphology is predominatly rod like, which however tends to spheroidize with continued ageing. The $Mn_{12}si_7Al_5$ phase precipitates at the austenite/ferrite boundary at all ageing temperatures.

References

1. J. C. BENZ and H. W. LEAVENWORTH, *J. Metals* **37** (1985) 36.
2. K. N. RAO, R. SHIVAKUMAR and M. L. BHATIA, *Trans. Indian Inst. Metals*, **39** (1986) 175.
3. A. INOUE, Y. KIJIMA, T. MINEMURA and T. MASUMOTO, *Metall. Trans. A* **12A** (1981) 1245.
4. G. E. HALE, PhD thesis, Department of Metallurgy, University of Leeds, Leeds (1982).
5. W. K. CHOO and K. H. HAN, *Metall. Trans. A.* **16A** (1985) 5.
6. K. H. HAN and W. K. CHOO, *ibid.* **14A** (1983) 973.
7. G. L. KAYAK, *Met. Sci. Heat Treatment* **11** (1969) 95.
8. G. S. KRIVONOGOV, M. F. ALEKSEYENKO and G. G. SOLOV'YEVA, *Phys. Met. Metall.* **39** (1975) 86.
9. S. K. BANERJI, in Workshop on Conservation and Substitution Technology for Critical Applications, Vanderbilt University, Nashville, Tenessee, USA, June, 1981.
10. N. A. STORCHAK and A. G. DRACHINSKAYA, *Phys. Met. Metall.* **44** (1978) 121.
11. M. F. ALEKSEENKO *et al., Met. Sci. Heat Treatment* **14** (1972) 187.
12. T. F. LIU and C. M. WAN, *Scripta Metall.* **19** (1985) 727.
13. *Idem., ibid.* **19** (1985) 805.
14. A. PRODHAN, PhD thesis, Metallurgical Engineering Department, I. I. T., Kharagpur, India (1988).
15. J. TASKAR, in Proceedings of 28th SCRATA Conference 1983 (Steel Castings Research and Trade Association, 1983) Paper 15.
16. J. B. DUH, W. T. TSAI and J. T. LEE, *Scripta Metall.* **21** (1987) 95.
17. G. E. DIETER, in "Mechanical Metallurgy", 2nd edn (McGraw Hill, Kogakusha Ltd, 1976) p. 162.

Received 11 October 1988
and accepted 10 April 1989